



This is a repository copy of *Evaluation of hydrogen permeation in fretting corrosion interfaces with Ti-6Al-4V alloy and varying lubricants using a modified Devanathan-Stachurski cell.*

White Rose Research Online URL for this paper:

<https://eprints.whiterose.ac.uk/220927/>

Version: Published Version

Article:

Khan, T. orcid.org/0000-0001-9621-9928, Beadling, A.R., Taufiqurrakhman, M. et al. (1 more author) (2024) Evaluation of hydrogen permeation in fretting corrosion interfaces with Ti-6Al-4V alloy and varying lubricants using a modified Devanathan-Stachurski cell. *Tribology Transactions*, 67 (6). pp. 1147-1157. ISSN 1040-2004

<https://doi.org/10.1080/10402004.2024.2409193>

Reuse

This article is distributed under the terms of the Creative Commons Attribution-NonCommercial-NoDerivs (CC BY-NC-ND) licence. This licence only allows you to download this work and share it with others as long as you credit the authors, but you can't change the article in any way or use it commercially. More information and the full terms of the licence here: <https://creativecommons.org/licenses/>

Takedown

If you consider content in White Rose Research Online to be in breach of UK law, please notify us by emailing eprints@whiterose.ac.uk including the URL of the record and the reason for the withdrawal request.



eprints@whiterose.ac.uk
<https://eprints.whiterose.ac.uk/>



Evaluation of Hydrogen Permeation in Fretting Corrosion Interfaces with Ti-6Al-4V Alloy and Varying Lubricants Using a Modified Devanathan-Stachurski Cell

Thawhid Khan, Andrew Robert Beadling, Mohamad Taufiqurrakhman & Michael G. Bryant

To cite this article: Thawhid Khan, Andrew Robert Beadling, Mohamad Taufiqurrakhman & Michael G. Bryant (2024) Evaluation of Hydrogen Permeation in Fretting Corrosion Interfaces with Ti-6Al-4V Alloy and Varying Lubricants Using a Modified Devanathan-Stachurski Cell, Tribology Transactions, 67:6, 1147-1157, DOI: [10.1080/10402004.2024.2409193](https://doi.org/10.1080/10402004.2024.2409193)

To link to this article: <https://doi.org/10.1080/10402004.2024.2409193>



© 2024 The Author(s). Published with license by Taylor & Francis Group, LLC



Published online: 11 Nov 2024.



Submit your article to this journal [↗](#)



Article views: 210




View related articles [↗](#)



View Crossmark data [↗](#)

Evaluation of Hydrogen Permeation in Fretting Corrosion Interfaces with Ti-6Al-4V Alloy and Varying Lubricants Using a Modified Devanathan-Stachurski Cell

Thawhid Khan^a , Andrew Robert Beadling^b, Mohamad Taufiqurrakhman^b, and Michael G. Bryant^b

^aInstitute of Functional Surfaces, Mechanical Engineering, University of Leeds, Leeds, Yorkshire, UK; ^bSchool of Mechanical Engineering, University of Birmingham, Edgbaston, West Midlands, UK

ABSTRACT

Titanium alloys are commonly used in biomedical applications for structural components such as hip femoral stems and acetabular cup shells. Whilst the fretting-corrosion degradation of titanium (Ti)-alloys has been well documented, the role of hydrogen permeation within these contacts has not received much attention despite evidence in clinical retrieval studies. This is likely due to the complexity of measurement and simulation. The aim of this study was to better understand the effect of tribological and electrochemical mechanisms on hydrogen permeation. A novel detection cell based on the Devanathan-Stachurski (DS) cell was designed to investigate hydrogen permeation in fretting corrosion contacts found in titanium-aluminum-vanadium (Ti-6Al-4V) alloy. Hydrogen permeation was found to be dependent on the amplitude of fretting displacement. Hydrogen permeation was not detected at lower amplitudes (10 and 50 μm); whereas, a significant increase in hydrogen permeation was found at 150 μm displacements. Furthermore, hydrogen permeation was found to be affected by the components of the tested physiological saline solution. Presence of hydrogen permeation was noticed in 0.9% sodium chloride (NaCl) and physiological saline combined with albumin protein. However, the amount of permeated hydrogen was reduced (38%) when hydrogen peroxide (H_2O_2) was added. While corrosion rate and hydrogen permeation increased (6%) significantly when both albumin and H_2O_2 were added to the solution. These results show that fretting induced hydrogen ingress can be simulated and detected in situ within simulated aqueous environments. Furthermore, a framework to assess the interactions between fretting and hydrogen ingress, which can be translated to other industrial challenges, has been developed.

ARTICLE HISTORY

Received 1 February 2024
Accepted 20 September 2024

KEYWORDS

Ti-6Al-4V; Devanathan-Stachurski cell; fretting-corrosion; hydrogen permeation

Introduction

Titanium-based alloys have gained significant attention in various industries due to their exceptional mechanical properties, low density, and excellent corrosion resistance. These alloys find extensive applications in critical components such as aerospace structures, gas turbines, and biomedical implants. However, despite their remarkable characteristics, titanium alloys are susceptible to certain challenges, including hydrogen ingress and fretting fatigue, which can compromise their structural integrity and performance. (1,2)

Hydrogen ingress, the diffusion of atomic hydrogen into the alloy matrix, poses a substantial concern in titanium-based alloys. The presence of hydrogen can significantly affect their mechanical properties, leading to embrittlement, reduced fatigue life, and catastrophic failures. Hydrogen embrittlement is particularly critical in applications involving high-stress environments, where the presence of hydrogen atoms at titanium lattice sites can alter the alloy's dislocation movement and fracture behavior. The

interactions between fretting and hydrogen embrittlement have been long established; the acting mechanisms quantified through systematic materials characterization techniques. The localized surface damage caused by fretting can initiate cracks, leading to fatigue failure even under relatively low applied stresses. When combined with hydrogen ingress, fretting can accelerate crack propagation, exacerbating the overall degradation process of the material. (3–5)

Titanium based alloys have found extensive application within the biomedical device domain in various physiological solutions. (6) In physiological environments the alloy forms a thin, dense, and nearly stoichiometric titanium dioxide (TiO_2) oxide layer on the surface, thereby enhancing the components corrosion resistance. (7) The effect of corrosion, wear, and the combined synergetic effect of both have been emphasized as the predominant reason for implants degradation. However, the exact mechanisms of degradation are still unclear. (8) Rodrigues et al. (9) reported severe in vivo corrosion and hydrogen embrittlement of titanium-aluminum-vanadium (Ti6Al4V-

CONTACT Thawhid Khan  thawhidkhan@yahoo.co.uk
Review led by B. Gould.

© 2024 The Author(s). Published with license by Taylor & Francis Group, LLC
This is an Open Access article distributed under the terms of the Creative Commons Attribution-NonCommercial-NoDerivatives License (<http://creativecommons.org/licenses/by-nc-nd/4.0/>), which permits non-commercial re-use, distribution, and reproduction in any medium, provided the original work is properly cited, and is not altered, transformed, or built upon in any way. The terms on which this article has been published allow the posting of the Accepted Manuscript in a repository by the author(s) or with their consent.

Ti6Al4V) hip modular taper interfaces. Titanium hydride (TiH) formation, surface reaction, and cracking within the modular interfaces was observed indicating the co-existence and synergistic interaction between tribology, corrosion and hydrogen ingress processes. Hydrogen embrittlement has also been implicated on early fracture and failure of dental, spinal and cardiovascular stents; all of which have a contacting fretting interface in common.

Common tests to assess the corrosion behavior of biomedical alloys are typically conducted in solutions like physiological saline (0.9% sodium chloride [NaCl]) (10) or phosphate-buffered saline (PBS). (11) However, within a peri-implant environment biological species such as albumin proteins and reactive oxygen species (ROS) such as hydrogen peroxide (H_2O_2) (12,13) can modify corrosion behavior. There are limited studies that have extensively investigated the effects of these species in combination and in a tribocorrosion environment. (14) No studies to date have addressed the effect of lubricant chemistry of H_2 ingress.

This study will replicate the fretting behavior commonly observed within orthopedics between cobalt-chromium-molybdenum (CoCrMo) femoral heads and Ti-alloy femoral stems via a modular taper connection (15). When this material combination has been used in a metal-on-metal total hip replacement scenarios, unacceptably high revisions rates have been observed due to degradation at the CoCrMo-Ti-alloy modular taper interfaces. The degradation has been attributed to a fretting fatigue, hydrogen embrittlement or tribocorrosion mechanisms. (16)

To effectively address the challenges associated with hydrogen ingress and fretting in titanium-based alloys, a comprehensive understanding of the underlying mechanisms, including the interaction between hydrogen atoms and the alloy matrix, as well as the complex tribological phenomena occurring during fretting, is required. To achieve this, new methodologies are required that enable in situ and real-time assessment of H_2 ingress during tribological processes. In this paper, we present the design and development of a novel methodology, based on the Devanathan-Stachurski (DS) cell, to investigate the role of fretting-corrosion on H_2 ingress. This novel cell replaces the charging-corrosion side of a conventional cell with a “lubricated rubbing” device that allows the H -permeation to be recorded on the

detection side and for the effect of different lubricants on hydrogen permeation into titanium to be investigated. We aim to better understand the mechanisms driving these phenomena through by interrogating the roles of slip magnitude and environment on hydrogen evolution.

Cell design and manufacture

The DS cell is an electrochemical cell used to measure the diffusion coefficient of hydrogen in a solid material. It consists of three main components: a solid membrane (Ti6Al4V), two electrode compartments (in this case, tribo and diffusion side), and a source of hydrogen (lubricant). The hydrogen flux is directly proportional to the partial pressure gradient across the membrane and can be quantified using Fick's law of diffusion. By measuring the current passing through the cell and knowing the thickness and area of the membrane, the diffusion coefficient of hydrogen in the solid electrolyte can be determined. The cell consisted of three main parts; the bottom base to contain the detection cell, the top plate which houses the sample with the charging cell and the fixing plate which secures the sample to the top plate. The depth of the bath was 30.2 mm that allows the insertion of the charging cell and the immersion of the electrolytic solution, while also giving a thickness of 7.8 mm at the bottom to increase durability. The base had a wall thickness of 3.8 mm to be able to withstand any high loading applied without cracking.

The fixing plate had a circular shape with four extruded M3 screw slots originated at a 90° angle between each slot and covering the border of the plate. Figure 1A represents the fixing plate. In the center of the plate, there is a hole that allows contact between the ball and the sample. Moreover, the thickness of the plate was 4.8 mm whereas the screw slots had a 2.5 mm clearance. This was created a lip sealing mechanism to secure the titanium sample onto the top plate Fig. 1B.

The top plate was designed to be inserted inside the bottom base. The bath had 18 mm of depth and 68 mm of width, to provide space to insert the ball and its fixing mechanism to be in contact with the Ti sample. Furthermore, there was a slot that allows the insertion of the electrode into the detection cell

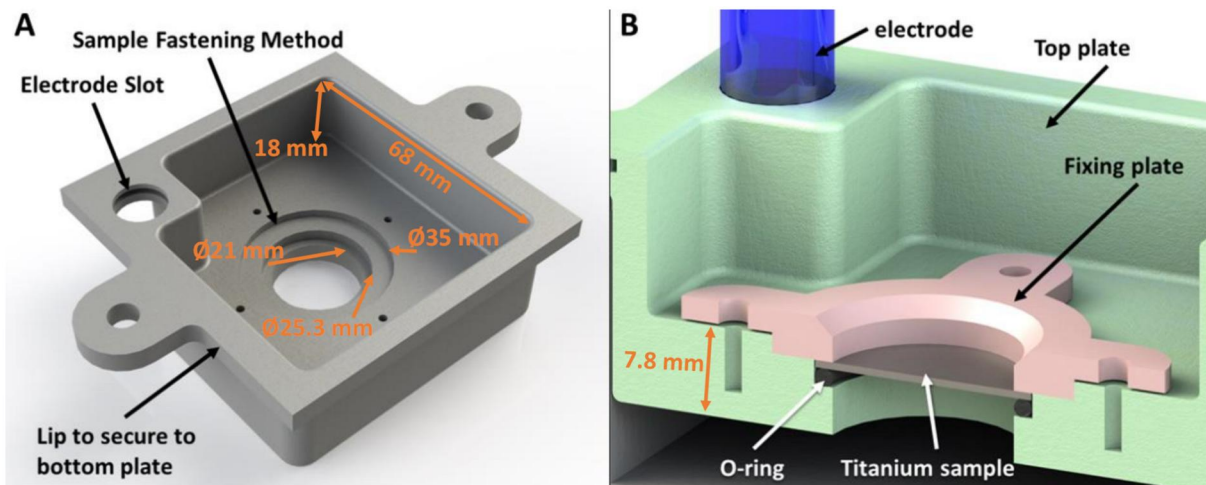


Figure 1. (A) Isometric 3D render of the top plate. (B) Section view illustrating the fastening mechanism (colors were changed for demonstration purposes).

in the bottom. Figure 1B provides a 3D render of the top plate illustrating the main features. Finally, at the bottom of the plate, there was the fastening mechanism of the titanium sample. The mechanisms consist of a hole tapered in three stages as follows; the first stage was a 35 mm in diameter circular cut with 2 mm depth. This was modeled to attach the fixing plate. The second stage was 25.3 mm circular cut with 2.8 mm depth, this part allows inserting the titanium sample over a 2 mm O-ring. The O-ring was added to ensure the lubricant used in the charging cell do not leak to the detection cell below. The load applied from the cantilever which will be elaborated in further sections was used to press the O-ring and seal it in position. The final stage was a 21 mm circular cut with 5.2 mm depth that allows the titanium sample to be in contact with the electrolytic solution in the detection cell. Figure 1B illustrates the fastening mechanism of the titanium sample.

The DS cell parts were manufactured using a 3D printer and white photopolymer material. This photopolymer is appropriate for the fretting corrosion environment of the test, given that virgin wood particle (VWP) is nonconductive and can withstand considerable amounts of loading.

Materials and methodology

Materials

CoCrMo balls and Ti6Al4V plate samples have been utilized in this study. This materials combination is common in total hip arthroplasty and can be found in modular taper trunnions (i.e., femoral head-femoral stem), acetabular liner-acetabular shell and femoral stem-neck taper connections. Wrought Ti6Al4V membrane samples were prepared from Ø25 mm diameter bar stock and cut to 0.8 ± 0.05 mm thickness using electrical discharge machining. Prior to each test the sample was polished to 1000-grit silicon carbide grinding paper. After polishing the sample was rinsed with Ethanol and dried using an air compressor to eliminate any debris and polishing remains. A Ø28 mm low carbon CoCrMo sphere ($R_a \approx 10$ nm) was used as the counter surface. A combined silver/silver chloride (Ag/AgCl) reference electrode (RE) and Pt (CE) was used to complete the 3-electrode electrochemical cell. The Ti-alloy plate and CoCrMo formed the working electrode (WE).

In this study, four lubricants were used assessed to observe the role of environment on hydrogen permeation. All reagents were purchased commercially and used as received. Table 1 outlines the lubricants and rationale and 25 mL of each lubricant was used in the tribo-cell.

Methodology

After assembling, the DS cell was attached to a bespoke fretting rig with a ball on plate configuration. The fretting rig was custom made at School of Mechanical Engineering, University of Leeds, UK. Details of the fretting instrument can be found in Oladokun et al. (17) Figure 2 shows a schematic of the fretting rig with the attached DS cell. Fretting was simulated by applying micro-motion to the Ø28 CoCrMo ball relative to the Ti6Al4V plate under a dead weight normal load. This would replicate the fretting behavior at the CoCrMo-Ti-alloy modular taper interfaces. The applied cyclic displacement and resultant tangential forces were captured at 200 Hz and analyzed as per the frameworks presented by Fouvry et al. (18)

Two distinct fretting experiments were carried out in this study, where tangential force, energy dissipation, current density, and permeated H_2 were measured with each experiment.

1. **Varying displacement on hydrogen permeation:** Experiment 1 involved using 0.9% NaCl solution and the fretting test parameters highlighted in Table 2 at three varying displacements: 10, 50, and 150 μ m, to target different fretting regimes. Each displacement was tested two times for reproducibility. Given that the anodic current decays exponentially until reaching steady state, the cell was left static for 3600 s to reach steady state before the fretting test was initiated.
2. **Varying lubricants on hydrogen permeation:** Experiment 2 used the same fretting conditions as Experiment 1; however, sliding displacement was fixed to 150 μ m and four lubricant variants were utilized as highlighted in Table 1. Each lubricant was tested at least three times for reproducibility.

An automated system was used to control and record the electrochemical reactions. The potentiostat was connected to, and controlled by, computer software. In this study, the anodic potential was applied to the diffusion compartment, using a constant overpotential equal to 400 mV versus Ag/AgCl. The resultant net anodic current of the Ti-alloy surface on the diffusion cell side (i.e., non-tribo contact) was captured at 1 Hz. Anodic current is measured as it is directly proportional to the amount of hydrogen permeating through the sample with time. (19) The electrolyte in the diffusion compartment was 0.2 M NaOH concentration.

The current density (μ A/cm²) was calculated by dividing the anodic current by the exposed area of the Ti sample to

Table 1. Lubricants chosen for this study.

Lubricant	Description	Rationale
A	0.9% sodium chloride	Isotonic saline solution. Commonly used in standards testing
B	0.9% sodium chloride with 0.1% bovine serum albumin (BSA)	Isotonic saline solution with addition of organic species.
C	0.9% sodium chloride with 0.1% hydrogen peroxide (H ₂ O ₂)	Simple simulated inflammatory environment. Modified corrosion reduction half-cell reaction.
D	0.9% sodium chloride with 0.1% bovine serum albumin (BSA) and 0.1% hydrogen peroxide (H ₂ O ₂)	Isotonic saline solution with addition of organic species. To investigate the role of simulated inflammation in presence of albumin species.

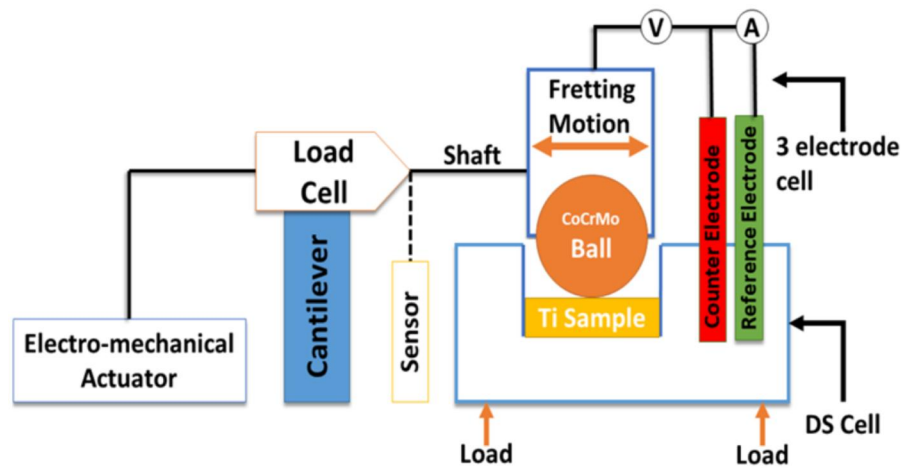


Figure 2. Schematic of the fretting corrosion rig with Devanathan-Stachurski (DS) cell.

Table 2. Fretting test parameters utilized in this study.

Load (N)	35
Contact Pressure (MPa)	594
Displacement (μm)	10, 50, and 150
Frequency (Hz)	1
Cycles	10,800
	3,600 static, 3,600 fretting and 3,600 static
Anodic Potential (mV)	400

the electrolytic solution. The exposed area was found equal to 3.46 cm^2 . Hence, the amount of permeated hydrogen (P) was calculated using Eq. [1].

$$P = \frac{1}{Ft} \int_0^t J dt \quad [1]$$

where, F is Faraday's Constant (96.485 C/mol), t is the integration time, and J is the hydrogen oxidation current density (A/cm^2).

Results

Fretting loops & energy dissipation

Figure 3 shows the fretting loops for both experiments and the dissipated energy per cycle. For the fretting loops, each test loops were averaged and plotted against the average tangential force (F_t).

Varying displacement

Figure 3A shows the average fretting loops of Experiment 1. The fretting loops illustrated an expected regime for each selected displacement (20); a stick regime was shown with $10 \mu\text{m}$ displacement illustrating a closed and narrow loop. A quasi-stick profile was illustrated with the partial slip $50 \mu\text{m}$ displacements. (21,22) Correspondingly, $150 \mu\text{m}$ displacements had a parallelogram shape demonstrating a gross slip regime. However, subtle deviations were noticed in the 50 and $150 \mu\text{m}$ fretting loops when compared to a typical partial-slip and gross slip profiles as seen in the literature. (20) This might be resulted from either the slipping occurring due to wear generation in the region or due to some experimental errors such as movements

occurring to the Ti sample during the fretting test. Liu et al. (23) found similar trends and believed it was due to the imperfections on the surface finish of the fretting samples. Fantetti et al. (24) showed a significant change to gross slip hysteresis loops due to wear over time, with both friction coefficient and contact stiffness also noticeably influenced by the wear evolution.

The energy dissipated (E_d) per cycle was plotted in Fig. 3B. For Experiment 1, the dissipated energy values for a stick regime ($10 \mu\text{m}$) were significantly minimal with an average of $0.002 \times 10^{-3} \text{ J}$. The partial slip ($50 \mu\text{m}$) had a slightly higher amount of energy with $0.4 \times 10^{-3} \text{ J}$ average. However, there was a significant difference in energy dissipation with the gross slip regime ($150 \mu\text{m}$) when compared to the first two tests ($2.86 \times 10^{-3} \text{ J}$).

Varying lubricant

Similar analysis was carried out for Experiment 2. Fretting loops for the four tested lubricants are illustrated in Fig. 3C. There was a noticeable difference in the fretting loops of each lubricant although the displacement was fixed to $150 \mu\text{m}$ for all tests. Lubricant B had the smallest loop illustrating lower tangential forces. Correspondingly, Lubricant A illustrated higher amounts of dissipated energy, the average fretting loop was noticeably larger due to higher tangential forces while having less mismatch in displacement. Lubricant C had the largest loop indicating higher tangential forces. Moreover, lubricants C and D both had the largest amount of slipping as shown in Fig. 3C, while lubricant C had more slipping at the edges of the loop.

In terms of dissipated energy for Experiment 2, the averaged dissipated energy for each lubricant was plotted in Fig. 3D. As expected from the fretting loops plot (Fig. 3C) lubricant B had the lowest amount of dissipated energy with an average of $2.17 \times 10^{-3} \text{ J}$. However, the main differences were noticed in lubricants C and D. Lubricant C had the largest fretting loop and also illustrated higher amounts of dissipated energy ($4.51 \times 10^{-3} \text{ J}$) than lubricant D ($3.37 \times 10^{-3} \text{ J}$).

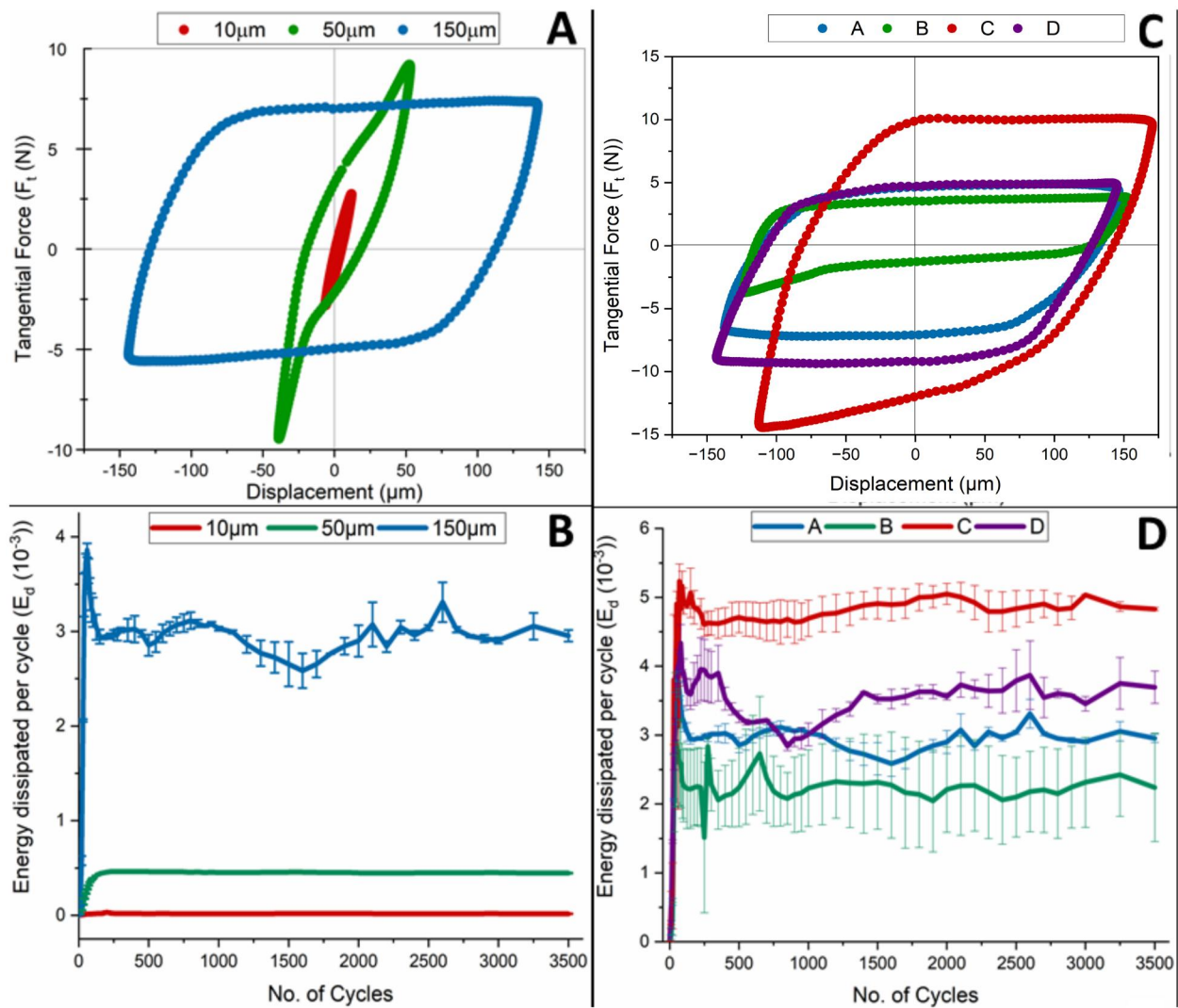


Figure 3. Fretting of Ti-6Al-4V-CoCrMo: (A) fretting loops of Experiment 1 while varying displacement. (B) Energy dissipated per cycle for Experiment 1. (C) Fretting loops of Experiment 2 with 150 μm displacement submerged in different lubricants. (D) Energy dissipated for Experiment 2. Data shown in (B) and (D) are mean $\pm 95\%$ confidence intervals.

Hydrogen permeation current density

Varying displacement

Figure 4A illustrates the measured current density values for the three varying displacements for Experiment 1. There was no significant increase in both 10 and 50 μm displacements tests. The current density i decayed exponentially to a baseline current without any fluctuations for the duration of the test. However, higher displacements of 150 μm were found to have a significant increase in current density as soon as fretting was started at 3600 s. With the 150 μm displacement tests, the average current density value was 4.77 $\mu\text{A}/\text{cm}^2$. As a result, only 150 μm was selected for Experiment 2 to investigate the four different lubricants.

Varying lubricant

With Experiment 2 (Fig. 4B) each lubricant was tested twice. First, lubricant C demonstrated the lowest increase in current density at the onset of sliding, with average value equaled 3.26 $\mu\text{A}/\text{cm}^2$ during the fretting cycle. However, it

had higher baseline values before initiating the fretting test as illustrated in Fig. 4B.

Second, for lubricant A and B, the hydrogen current illustrated higher values during fretting when compared to lubricant C. Higher current density values proved that more amounts of hydrogen were passed through the Ti sample during fretting. Also, the baseline values before fretting begun for both tests were significantly lower than lubricant C. However, the baseline for lubricant B was higher than lubricant A. The environment in lubricant A and B seemed less corrosive as higher current density values were observed when fretting begun illustrating that hydrogen atoms generated in the charging cell were able to passivate through the Ti sample.

Finally, lubricant D current density illustrated a different behavior from a typical fretting current density plot. Lubricant D current had not yet achieved steady state prior to the fretting test. The current density was seen to continue in decaying and appeared unaffected from the fretting cycle as expected.

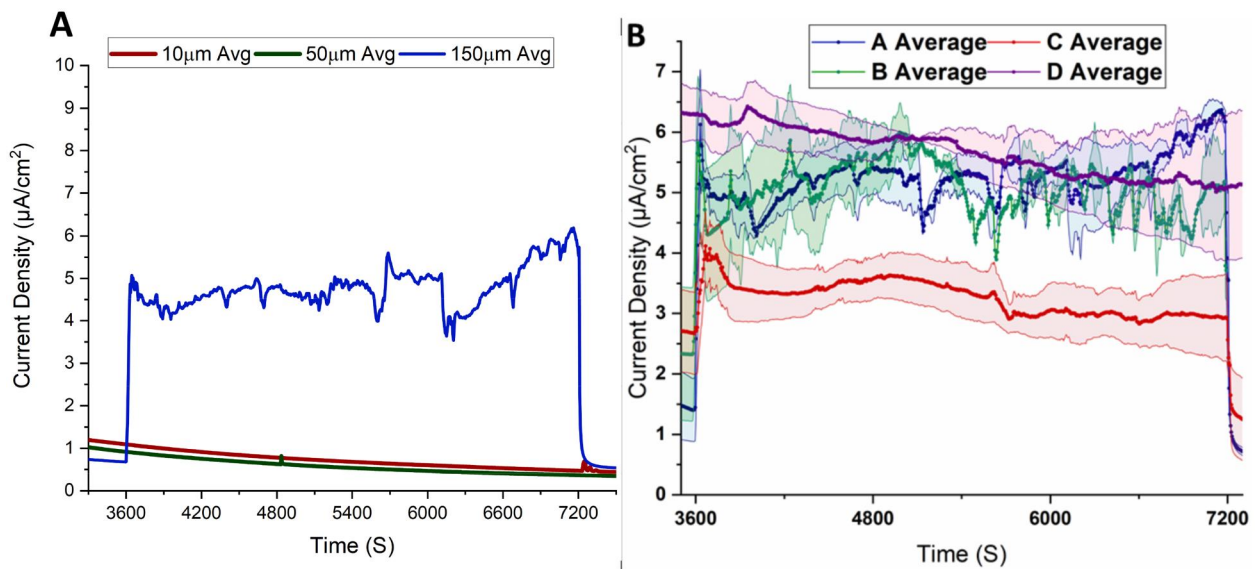


Figure 4. (A) Current density against time for the three selected displacements. (B) Mean $\pm 95\%$ confidence intervals of current density for different lubricants through the fretting cycle.

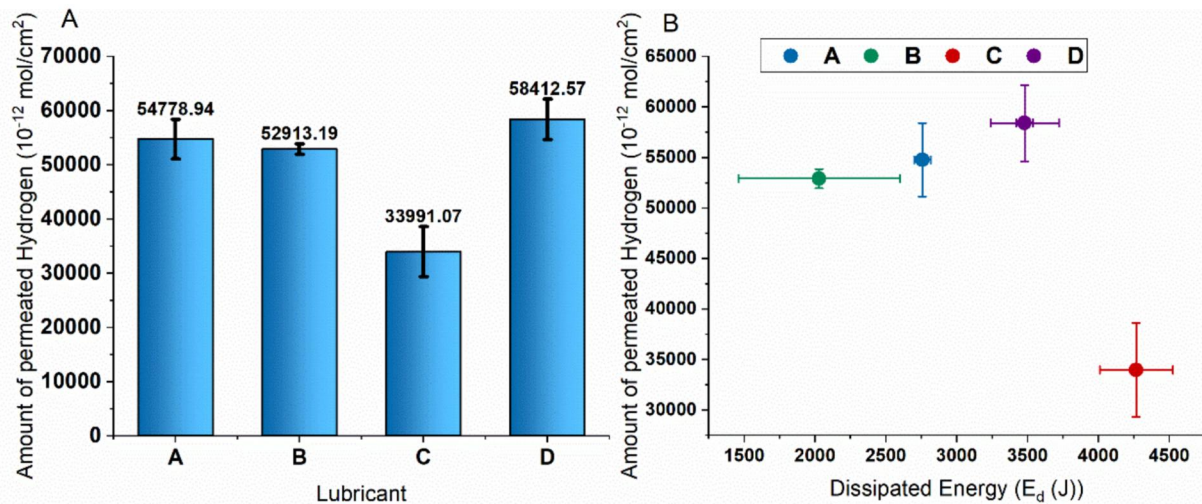


Figure 5. (A) Amount of permeated hydrogen for each lubricant (B) hydrogen permeation plot against dissipated energy. Data shown are mean $\pm 95\%$ confidence intervals.

Hydrogen permeation

The amount of permeated hydrogen with the varying lubricants from Experiment 2 was calculated by integrating the current density graphs during fretting. Hence, the values were incorporated into Faraday's law (Eqs. [2]–[4]). For each lubricant, the mean value of hydrogen permeation was calculated with 95% confidence intervals of the two repeats. The averaged values were hence plotted in Fig. 5A. Also, hydrogen permeation was plotted against the dissipated energy (E_d) (Fig. 5B) obtained from the averaged fretting loops (Fig. 3C). Higher values of hydrogen permeation were noted in lubricant A and B with significantly less dissipated energy. Both lubricants (A and B) illustrated a typical fretting current density trends (Fig. 4B), even though the anodic current is not measured due to overpotential and sliding wear as done in other studies suggesting a direct link between microscale contact perturbations and H_2 ingress.

Nevertheless, lubricant C had the lowest amount of hydrogen permeation with the highest amount of energy dissipation between the four lubricants. The calculated amounts of permeated hydrogen were significantly higher when integrating the fretting area for lubricant D. The current density for lubricant D (Fig. 4B) was significantly high before fretting began and did not increase or stabilize once fretting did start instead it continued to decay over time. Moreover, the amount of permeated hydrogen for lubricant D was 6% and 9.5% higher than lubricant A and B, respectively. While the dissipated energy for lubricant D was 35% and 52% higher than lubricant A and B, respectively.

Discussion

For in-vitro conditions Titanium alloys demonstrate excellent corrosion resistance. However, in-vivo with the

exposure to tissues the corrosion resistance of titanium implants can deteriorate. This is due to the presence of superoxide anions (ROS) and H_2O_2 caused by inflammation around the peri-implant tissue. It is hypothesized that in-vitro implants undergo a simultaneous action of corrosion and wear which can damage the protective oxide layer present on the implant. Alongside this the influence of ROS and proteins individually or in synergy can lead to further degradation of the implant. (8) Although implant retrieval analysis shows hydrogen permeation to date, methods to assess this in situ and in real-time are limited. The aim of this study was to develop a methodology that would enable quantification of H_2 permeation in real-time. To this end, a methodology that utilizes a bespoke DS integrated within a fretting tribometer arrangement has been developed. This combination allows for tribology and electrochemical processes to be quantified and synchronized.

Role of slip on H_2 permeation

With Experiment 1, traditional fretting loop behaviors were observed (Fig. 3A) with the varying displacement and matched the expected fretting regimes as highlighted by the literature. (25) Other studies, including those conducted by the authors for the same materials couples, loading and slip conditions, have found that higher energy dissipation suggested a higher likelihood of wear. (16,26–30) Low and consistent current density measurements (varying between 1.3 and $0.5 \mu A/cm^2$) (Fig. 4A) was observed at the 10 μm and 50 μm displacements. However, with the 150 μm displacement tests a significant increase (varying between 4.5 and $5.5 \mu A/cm^2$) was observed and this corresponded with higher energy dissipation (Fig. 3B). This increase in energy was also accompanied by higher amounts of hydrogen permeation. This indicated that the slip mechanism potentially defined H_2 ingress. Previous studies (31,32) have highlighted that hydrogen permeation occurs due to the tribological wearing occurring at the interface. Gross slip fretting regimes have been shown to exhibit the most significant wear (33,34) and from Fig. 3A it is possible to see at the higher displacement (150 μm) gross slip is occurring. Compared to other studies this DS cell allows the monitoring of real time H_2 permeation during tribological tests under fretting conditions. As a result, it can be assumed that a combination of nascent metal exposure, from the higher assumed wear occurring within the gross slip regime, to the lubricant would influence H_2 permeation. A limitation of this study is the test duration under partial slip conditions where aspects of crack propagation and fatigue will occur further contributing to H_2 ingress.

Role of lubricant type on H_2 permeation

The electrochemical current trends with the different lubricant variations (Experiment 2) from this study were similar to the behaviors observed by Gopal and Manivasagam (8) and Zhang et al. (35) who used the same lubricants with the exception of using a PBS instead of BSA as the base

solution. A key difference between this study and others (8,35) was that the current density is measured on the unworn underside of the Ti sample, which represents a shift in the net anodic current due to an increase in H^+ at the interface, whereas with the latter study it was measured on the fretting worn surface which was due to anodic oxidation. The hydrogen permeation current is directly related to the quantity of absorbed hydrogen and corresponds to the difference in hydrogen concentration between the membrane's entry side (at the surface) and the exit side, where the concentration is zero due to the applied positive potential. This study highlights how H_2 permeation plays an influential factor in wear and corrosion behavior with titanium alloys in different physiological simulated environments.

Lubricants A and B

During traditional fretting-corrosion studies, a variation in Open Circuit Potential and current density can be observed with varying lubricants which is caused by cyclic film depassivation and regeneration. (36) Similarly in this study, the role of lubricant was seen to influence the ingress of H_2 . Whilst lubricant A and B produced the highest total amount of H_2 permeated, albeit with little difference observed between the two lubricants, differences in the baseline current prior to slip were observed. Prior to slip, the addition of BSA increased the measured current within the detection cell indicating a higher hydrogen permeation. Although this study detects electrochemical transients within the charging cell, parallels with existing corrosion and tribocorrosion studies can be made in terms of the roles of BSA. Overall, the current density baselines for Lubricants A & B were the lowest before fretting begun, indicating low pure corrosion was occurring and therefore low hydrogen permeation. This indicates synergy between an increase in hydrogen permeation and the tribological interactions during fretting, which was supported by the findings of Esfahani et al. (31) who showed H_2 permeation was linked to tribological wearing.

The lower current density behavior observed during fretting when using a combination of NaCl + BSA (lubricant B) in-comparison to just NaCl solution (lubricant A) was similar to observed by Liams et al. (9) It is believed that the slightly lower current density with the BSA solution was due to its molecules adsorbing on to the titanium surface that would inhibit the rate of oxygen cathodic reactions and move the corrosion potential toward more cathodic levels. (37) Karimi and Alfantazi (38) highlighted similar trends to this study where BSA was found to enhance the corrosion of Ti alloy before fretting occurred in-comparison to the NaCl solution hypothesizing BSA may deteriorate the oxide film stability and encouraged corrosion. This may indicate that corrosion, tribocorrosion and H_2 ingress are intrinsically linked and affected by the nature of surface adsorbed layers. (39)

In this study BSA individually (lubricant B) demonstrated high current density and the lowest tangential forces, indicating the wear mechanism was more corrosion dominated than mechanical. While the lubricant with BSA had the lowest tangential force there was significant slipping occurring

at the edges (Fig. 3C). This behavior may be due to albumin being known to form a thin layer on the surface of the sample. (40)

Lubricant C

Lubricant C, which was NaCl + H₂O₂, had a higher baseline current prior to the application of fretting when compared to lubricants A + B. Interestingly, upon the application of fretting, the synergy between mechanical and H₂ ingress was not as significant, when compared to lubricants A and B suggesting the addition of H₂O₂ inhibits the fretting induced H₂ permeability synergy.

Similar behavior was observed by Zhang et al., (35) and it was believed H₂O₂ increases the corrosion rate of the Ti alloy and increased corrosion can lead to an increase in H₂ permeation. (39) Corrosion could be generated from the H₂O₂ decomposed products reacting with the Ti free ions liberated from the interface and free hydrogen atoms found in the environment. (41) The overall low current density behavior observed during fretting with NaCl + H₂O₂ (lubricant C) compared to the other lubricants can be due to the depassivation/repassivation behavior when it interacts with the Titanium alloy. The low-density current indicates that the repassivation rate was significant compared to the depassivation rate due to the strong oxidizing nature of H₂O₂. It is believed that after depassivation there is an instantaneous regrowth of the oxide layer which would help to reduce corrosion and act as a barrier reducing H₂ permeation, whereas with the NaCl (lubricant A) and NaCl + BSA (lubricant B) solutions the depassivation and repassivation rate is balanced and in a state of equilibrium. (10) Similar behaviors were observed by Ratoi et al. (42) supporting the hypothesis that even though large amounts of hydrogen can be generated in a hydrogen environment, a specific chemical tribofilm formation or layer presence can prevent its subsequent diffusion into the substrate during the tribological wearing process, which may explain the synergist observations for Lubricant C had the lowest hydrogen permeation.

This continuous behavior of depassivation and repassivation can lead to the formation of oxidized wear debris that may become embedded between the fretting components. (8) Several studies have shown that the presence of H₂O₂ (lubricant C) causes the highest wear, (15,43,44) where it is believed H₂O₂ causes a significant increase in metal release compared to NaCl or PBS base solution. The lower current density but higher tangential forces when H₂O₂ is present may indicate the wear with this lubricant is mechanically dominated.

Lubricant D

A higher current density is observed when using a combination of H₂O₂ and BSA lubricant (lubricant D) in-comparison to just H₂O₂ (lubricant C). Zhang et al. (35) found this corresponded with the formation of a thin corrosion product layer on the titanium component, which would lead to increased H₂ presence and permeation from the surface. It is believed BSA promotes dissolution of the peroxide

corrosion product layer. Sousa et al. (45) studied the interaction of BSA with a peroxide corrosion layer from a kinetic perspective of the BSA adhesion, adsorption and desorption. The research revealed that the hydrophilic surface of TiO₂, following immersion in H₂O₂, exhibited reduced albumin adsorption. Studies have shown that albumin can inhibit the corrosion of Ti alloys. (46–48) However, it demonstrated a higher work of adhesion, indicating a stronger attachment to the surface in comparison to the more hydrophobic sputtered TiO₂ surface. Following the adsorption phase, it was proposed that the exchangeability of albumin underwent temporal changes. Specifically, after 24 h, the albumin molecules adsorbed on the H₂O₂-treated TiO₂ surface appeared to be less readily exchangeable than those on the sputtered TiO₂ surface. However, after 72 h, nearly all the adsorbed albumin molecules effectively exchanged with others. This suggests that a longer duration is necessary for the exchange of albumin molecules adsorbed on the surface of H₂O₂-TiO₂ complexes. Consequently, the observed time-dependent dissolution behavior in the presence of this work aligns with the slow, rate-determining process of desorption of albumin-metal complexes, potentially resulting in thinner oxides. (35)

Berbel et al. (49) showed similar trends in the presence of H₂O₂ and BSA with the increase current density, which they believed gave a good indication of the aggressiveness of the solution toward the TiO₂ layer. Overall lubricant D had the highest hydrogen permeation prior to fretting, the baseline current density value was noticeably higher than the other fluids and over the duration of the testing, fretting seemed to have minimal impact on its trend. This suggests that the H₂O₂ and BSA lubricant (lubricant D) creates a severe corrosive environment through preventing the adsorption of albumin, (49) encouraging high H₂ permeation from the onset. It is believed the degradation of the Ti64 materials was mainly caused by H₂O₂ but was further enhanced by the presence of BSA. (50)

The two lubricants containing H₂O₂ (lubricants C & D) had the lowest current densities and the highest energy dissipations and tangential forces. The high tangential forces were combined with a considerable mismatch in displacements. This mismatch could be due to the generation of wear debris at the central region due to plastic deformation caused by the contact of asperities. This can result in the generated particles to shift near the edge of contact. Other studies have shown that these wear debris were hence oxidized, forming a thin layer at the Ti surface which contributes to the slipping occurring at the region. (51) A combination of increased tangential forces and higher energy dissipation with the presence of H₂O₂ indicate it would potentially have a detrimental effect on titanium implants.

Conclusions

The modified DS cell showed it can be used as a method for in-situ evaluation of different fretting regimes and aqueous environments in respect of their ability to generate

hydrogen. This cell measured the shift in net anodic current on the unworn underside of the Ti sample due to an increase H^+ at the fretting interface. The key conclusions drawn from the work are:

- Hydrogen permeation was found to be dependent on the amplitude of fretting displacement. At low fretting displacements (10 and 50 μm) hydrogen permeation was not detected, whereas at 150 μm a significant increase in hydrogen ingress was detected.
- There is a clear synergy between the tribological wear and the H_2 ingress. With the 0.9% (NaCl) and physiological saline combined with albumin protein lubricants, prior to fretting low hydrogen permeation was measured; however, with the on-set of tribological wearing, a significant increase in hydrogen ingress was measured.
- The formation of a specific chemical tribofilm formation or layer presence can prevent hydrogen diffusion into the titanium substrate during tribological fretting. With the addition of H_2O_2 to the NaCl lubricant there was a drop in hydrogen permeation by 38% and this is believed to be due to the formation of a protective layer.

Future work

This study serves as an initial yet valuable preliminary investigation into real-time monitoring of the effect of aqueous bio-environments on hydrogen generation. Future work will focus on in-depth wear and chemical analysis using techniques such as scanning electron microscope (SEM) with energy dispersive x-ray analysis (EDX). This would allow for wear mechanisms to be identified and the characterization of any protective layers formed. This approach will provide a deeper insight into the effect of the lubricant on friction and wear behavior alongside the ability of any formed layers to encourage or hinder hydrogen permeation. Ultimately, this expanded research will build upon the preliminary findings presented here, enhancing our understanding and leading to improved reproducibility and reliability in the real-time assessment of the effect of hydrogen permeation.

Acknowledgements

The authors would like to thank Mohammed Dawood for his contribution to the development and testing of the DS cell in this study.

Disclosure statement

The authors declare that they have no known competing financial interests or personal relationships that could have appeared to influence the work reported in this paper.

ORCID

Thawhid Khan  <http://orcid.org/0000-0001-9621-9928>

Data availability statement

Data will be made available on request.

References

- (1) Neikter, M., Colliander, M., de Andrade Schwerz, C., Hansson, T., Åkerfeldt, P., Pederson, R., and Antti, M.-L. (2020), "Fatigue Crack Growth of Electron Beam Melted Ti-6Al-4V in High-Pressure Hydrogen," *Materials*, **13**, 1287. doi:10.3390/ma13061287
- (2) Pakhomov, M., Gorlov, D., and Stolyarov, V. (2020), "Features of Wear and Friction in Titanium," *IOP Conference Series: Materials Science and Engineering*, **996**, 012017. doi:10.1088/1757-899X/996/1/012017
- (3) Asaoka, K., Yokoyama, K., and Nagumo, M. (2002), "Hydrogen Embrittlement of Nickel-Titanium Alloy in Biological Environment," *Metallurgical and Materials Transactions A*, **33**, pp 495–501. doi:10.1007/s11661-002-0111-8
- (4) Blau, P. J. (2014), "A Multi-Stage Wear Model for Grid-to-Rod Fretting of Nuclear Fuel Rods," *Wear*, **313**, pp 89–96. doi:10.1016/j.wear.2014.02.016
- (5) Kubota, M., Tanaka, Y., and Kondo, Y. (2009), "The Effect of Hydrogen Gas Environment on Fretting Fatigue Strength of Materials Used for Hydrogen Utilization Machines," *Tribology International*, **42**, pp 1352–1359. doi:10.1016/j.triboint.2009.04.006
- (6) Geetha, M., Singh, A. K., Asokamani, R., and Gogia, A. K. (2009), "Ti Based Biomaterials, the Ultimate Choice for Orthopaedic Implants – A Review," *Progress in Materials Science*, **54**, pp 397–425. doi:10.1016/j.pmatsci.2008.06.004
- (7) Gopal, V. and Manivasagam, G. (2020), "Wear – Corrosion Synergistic Effect on Ti-6Al-4V Alloy in H_2O_2 and Albumin Environment," *Journal of Alloys and Compounds*, **830**, 154539. doi:10.1016/j.jallcom.2020.154539
- (8) Liamas, E., Thomas, O. R. T., Muñoz, A. I., and Zhang, Z. J. (2020), "Tribocorrosion Behaviour of Pure Titanium in Bovine Serum Albumin Solution: A Multiscale Study," *Journal of the Mechanical Behavior of Biomedical Materials*, **102**, 103511. doi:10.1016/j.jmbbm.2019.103511
- (9) Rodrigues, D. C., Urban, R. M., Jacobs, J. J., and Gilbert, J. L. (2009), "In Vivo Severe Corrosion and Hydrogen Embrittlement of Retrieved Modular Body Titanium Alloy Hip-Implants," *Journal of Biomedical Materials Research Part B: Applied Biomaterials*, **88B**, pp 206–219. doi:10.1002/jbm.b.31171
- (10) RF, A. (1998), *Standard Practice for Corrosion Fatigue Testing of Metallic Implant Materials (F1801)*. Annual Book of ASTM Standards, Medical devices; Emergency Medical Services.
- (11) International, A. (2001), *ASTM: F2129-19a – Standard Test Method for Conducting Cyclic Potentiodynamic Polarization Measurements to Determine the Corrosion Susceptibility of Small Implant Devices*, ASTM International: West Conshohocken (PA).
- (12) Test, S. T. and Weiss, S. J. (1984), "Quantitative and Temporal Characterization of the Extracellular H_2O_2 Pool Generated by Human Neutrophils," *The Journal of Biological Chemistry*, **259**, pp 399–405. doi:10.1016/S0021-9258(17)43674-X
- (13) Mabillean, G., Bourdon, S., Joly-Guillou, M. L., Filmon, R., Baslé, M. F., and Chappard, D. (2006), "Influence of Fluoride, Hydrogen Peroxide and Lactic Acid on the Corrosion Resistance of Commercially Pure Titanium," *Acta Biomaterialia*, **2**, pp 121–129. doi:10.1016/j.actbio.2005.09.004
- (14) Yu, F., Addison, O., and Davenport, A. J. (2015), "A Synergistic Effect of Albumin and H_2O_2 Accelerates Corrosion of Ti6Al4V," *Acta Biomaterialia*, **26**, pp 355–365. doi:10.1016/j.actbio.2015.07.046
- (15) Semlitsch, M. (1987), "Titanium Alloys for Hip Joint Replacements," *Clinical Materials*, **2**, pp 1–13. doi:10.1016/0267-6605(87)90015-1
- (16) Oladokun, A., Hall, R. M., Neville, A., and Bryant, M. G. (2019), "The Evolution of Subsurface Micro-Structure and Tribo-Chemical Processes in CoCrMo-Ti6Al4V Fretting-Corrosion Contacts: What Lies at and Below the Surface?," *Wear*, **440–441**, 203095. doi:10.1016/j.wear.2019.203095
- (17) Oladokun, A., Pettersson, M., Bryant, M., Engqvist, H., Persson, C., Hall, R., and Neville, A. (2015), "Fretting of CoCrMo and

- Ti6Al4V Alloys in Modular Prostheses,” *Tribology-Materials, Surfaces & Interfaces*, **9**, pp 165–173. doi:10.1179/1751584X15Y.0000000014
- (18) Fouvry, S., Kapsa, P., and Vincent, L. (1996), “Quantification of Fretting Damage,” *Wear*, **200**, pp 186–205. doi:10.1016/S0043-1648(96)07306-1
- (19) DropSens, M. *Hydrogen Permeation with a Single Instrument According to ASTM G148*, https://www.metrohm.com/en_gb/applications/application-notes/autolab-applikationen-anautolab/an-ec-028.html
- (20) Wäsche, R. and Hartelt, M. (2014), “Fretting,” *Encyclopedia of Lubricants and Lubrication*, ed. T. Mang, pp 680–687. Springer: Berlin.
- (21) Llavori, I., Zabala, A., Urchegui, M. A., Tato, W., Aginagalde, A., Garate, I., and Gómez, X. (2018), “An Ad-Hoc Fretting Wear Tribotester Design for Thin Steel Wires,” *MATEC Web of Conferences*, **165**, 22018. doi:10.1051/mateconf/201816522018
- (22) Vincent, L., Berthier, Y., and Godet, M. (1992), “Testing Methods in Fretting Fatigue: A Critical Appraisal,” *Standardization of Fretting Fatigue Test Methods and Equipment*, *ASTM STP 1159*, ed. M. Helmi Attia and R. B. Waterhouse, pp 33–48, American Society for Testing and Materials: Philadelphia.
- (23) Liu, Y., Zhu, D., Pierre, D., and Gilbert, J. L. (2019), “Fretting Initiated Crevice Corrosion of 316LVM Stainless Steel in Physiological Phosphate Buffered Saline: Potential and Cycles to Initiation,” *Acta Biomaterialia*, **97**, pp 565–577. doi:10.1016/j.actbio.2019.07.051
- (24) Fantetti, A., Tamatam, L. R., Volvert, M., Lawal, I., Liu, L., Salles, L., Brake, M. R. W., Schwingshackl, C. W., and Nowell, D. (2019), “The Impact of Fretting Wear on Structural Dynamics: Experiment and Simulation,” *Tribology International*, **138**, pp 111–124. doi:10.1016/j.triboint.2019.05.023
- (25) Ma, L., Eom, K., Geringer, J., Jun, T.-S., and Kim, K. (2019), “Literature Review on Fretting Wear and Contact Mechanics of Tribological Coatings,” *Coatings*, **9**, 501. doi:10.3390/coatings9080501
- (26) Geringer, J., Forest, B., and Combrade, P. (2006), “Wear Analysis of Materials Used as Orthopaedic Implants,” *Wear*, **261**, pp 971–979. doi:10.1016/j.wear.2006.03.022
- (27) McCormack, B. A. O., Prendergast, P. J., and Gallagher, D. G. (1996), “An Experimental Study of Damage Accumulation in Cemented Hip Prostheses,” *Clinical Biomechanics*, **11**, pp 214–219. doi:10.1016/0268-0033(95)00076-3
- (28) Zhang, H., Brown, L. T., Blunt, L. A., Jiang, X., and Barrans, S. M. (2009), “Understanding Initiation and Propagation of Fretting Wear on the Femoral Stem in Total Hip Replacement,” *Wear*, **266**, pp 566–569. doi:10.1016/j.wear.2008.04.076
- (29) Fouvry, S., Kapsa, P., and Vincent, L. (1995), “Analysis of Sliding Behaviour for Fretting Loadings: Determination of Transition Criteria,” *Wear*, **185**, pp 35–46. doi:10.1016/0043-1648(94)06582-9
- (30) Kim, K. and Korsunsky, A. M. (2010), “Fretting Damage of Ni—MoS₂ Coatings: Friction Coefficient and Accumulated Dissipated Energy Evolutions. *Proceedings of the Institution of Mechanical Engineers, Part J: Journal of Engineering Tribology*, **224**, pp 1173–1180.
- (31) Esfahani, E. A., Morina, A., Han, B., Nedelcu, I., van Eijk, M. C. P., and Neville, A. (2017), “Development of a Novel in-Situ Technique for Hydrogen Uptake Evaluation from a Lubricated Tribocontact,” *Tribology International*, **113**, pp 433–442. doi:10.1016/j.triboint.2017.01.019
- (32) Lu, R., Minami, I., Nanao, H., and Mori, S. (2007), “Investigation of Decomposition of Hydrocarbon Oil on the Nascent Surface of Steel,” *Tribology Letters*, **27**, pp 25–30. doi:10.1007/s11249-007-9203-3
- (33) Kim, K. and Korsunsky, A. M. (2011), “Effects of Imposed Displacement and Initial Coating Thickness on Fretting Behaviour of a Thermally Sprayed Coating,” *Wear*, **271**, pp 1080–1085. doi:10.1016/j.wear.2011.05.013
- (34) Korsunsky, A. M. and Kim, K. (2010), “Dissipated Energy and Friction Coefficient Evolution during Fretting Wear of Solid Lubricant Coatings,” *Tribology International*, **43**, pp 861–867. doi:10.1016/j.triboint.2009.12.063
- (35) Zhang, Y., Addison, O., Yu, F., Troconis, B. C. R., Scully, J. R., and Davenport, A. J. (2018), “Time-Dependent Enhanced Corrosion of Ti6Al4V in the Presence of H₂O₂ and Albumin,” *Scientific Reports*, **8**, 3185. doi:10.1038/s41598-018-21332-x
- (36) Kumar, S., Narayanan, T. S. N. S., Ganesh Sundara Raman, S., and Seshadri, S. K. (2010), “Surface Modification of CP-Ti to Improve the Fretting-Corrosion Resistance: Thermal Oxidation vs. Anodizing,” *Materials Science and Engineering: C*, **30**, pp 921–927. doi:10.1016/j.msec.2010.03.024
- (37) Muñoz, A. I., and Mischler, S. (2015), “Electrochemical Quartz Crystal Microbalance and X-Ray Photoelectron Spectroscopy Study of Cathodic Reactions in Bovine Serum Albumin Containing Solutions on a Physical Vapour Deposition-CoCrMo Biomedical Alloy,” *Electrochimica Acta*, **180**, pp 96–103. doi:10.1016/j.electacta.2015.08.017
- (38) Karimi, S. and Alfantazi, A. M. (2014), “Ion Release and Surface Oxide Composition of AISI 316L, Co–28Cr–6Mo, and Ti–6Al–4V Alloys Immersed in Human Serum Albumin Solutions,” *Materials Science & Engineering. C, Materials for Biological Applications*, **40**, pp 435–444. doi:10.1016/j.msec.2014.04.007
- (39) Boiadjeva-Scherzer, T., Mirkova, L., Fafilek, G., Reinbold, J., Kronberger, H., Stache, H., Bodesheim, G., and Monev, M. (2022), “Hydrogen Permeation Through Steel during Cathodic Polarization of Lubricating Oils in a Modified Devanathan–Stachurski Cell,” *Scientific Reports*, **12**, 18662. doi:10.1038/s41598-022-21941-7
- (40) Jackson, D. R., Omanovic, S., and Roscoe, S. G. (2000), “Electrochemical Studies of the Adsorption Behavior of Serum Proteins on Titanium,” *Langmuir*, **16**, pp 5449–5457. doi:10.1021/la991497x
- (41) Tengvall, P., Lundström, I., Sjöqvist, L., Elwing, H., and Bjursten, L. M. (1989), “Titanium-Hydrogen Peroxide Interaction: Model Studies of the Influence of the Inflammatory Response on Titanium Implants,” *Biomaterials*, **10**, pp 166–175. doi:10.1016/0142-9612(89)90019-7
- (42) Ratoi, M., Tanaka, H., Mellor, B. G., and Sugimura, J. (2020), “Hydrocarbon Lubricants Can Control Hydrogen Embrittlement,” *Scientific Reports*, **10**, 1361. doi:10.1038/s41598-020-58294-y
- (43) Prestat, M. and Thierry, D. (2021), “Corrosion of Titanium under Simulated Inflammation Conditions: Clinical Context and in Vitro Investigations,” *Acta Biomaterialia*, **136**, pp 72–87. doi:10.1016/j.actbio.2021.10.002
- (44) Takemoto, S., Hattori, M., Yoshinari, M., Kawada, E., and Oda, Y. (2013), “Discoloration of Titanium Alloy in Acidic Saline Solutions with Peroxide,” *Dental Materials Journal*, **32**, pp 19–24. doi:10.4012/dmj.2012-194
- (45) Sousa, S. R., Moradas-Ferreira, P., Saramago, B., Melo, L. V., and Barbosa, M. A. (2004), “Human Serum Albumin Adsorption on TiO₂ from Single Protein Solutions and from Plasma,” *Langmuir: The ACS Journal of Surfaces and Colloids*, **20**, pp 9745–9754. doi:10.1021/la049158d
- (46) Ouerd, A., Alemany-Dumont, C., Berthomé, G., Normand, B., and Szunerits, S. (2007), “Reactivity of Titanium in Physiological Medium: I. Electrochemical Characterization of the Metal/Protein Interface,” *Journal of The Electrochemical Society*, **154**, C593. doi:10.1149/1.2769819
- (47) Contu, F., Elsener, B., and Böhni, H. (2002), “Characterization of Implant Materials in Fetal Bovine Serum and Sodium Sulfate by Electrochemical Impedance Spectroscopy. I. Mechanically Polished Samples,” *Journal of Biomedical Materials Research*, **62**, pp 412–421. doi:10.1002/jbm.10329
- (48) Karimi, S., Nickchi, T., and Alfantazi, A. (2011), “Effects of Bovine Serum Albumin on the Corrosion Behaviour of AISI 316L, Co–28Cr–6Mo, and Ti–6Al–4V Alloys in Phosphate

- Buffered Saline Solutions,” *Corrosion Science*, **53**, pp 3262–3272. doi:[10.1016/j.corsci.2011.06.009](https://doi.org/10.1016/j.corsci.2011.06.009)
- (49) Berbel, L. O., Banczek, E. d. P., Karousis, I. K., Kotsakis, G. A., and Costa, I. (2019), “Determinants of Corrosion Resistance of Ti-6Al-4V Alloy Dental Implants in an In Vitro Model of Peri-Implant Inflammation,” *PLoS One*, **14**, e0210530. doi:[10.1371/journal.pone.0210530](https://doi.org/10.1371/journal.pone.0210530)
- (50) Prestat, M., Vucko, F., Holzer, L., and Thierry, D. (2021), “Microstructural Aspects of Ti6Al4V Degradation in H₂O₂-Containing Phosphate Buffered Saline,” *Corrosion Science*, **190**, 109640. doi:[10.1016/j.corsci.2021.109640](https://doi.org/10.1016/j.corsci.2021.109640)
- (51) Gilbert, J. L. (2017), “Corrosion in the Human Body: Metallic Implants in the Complex Body Environment,” *Corrosion*, **73**, pp 1478–1495. doi:[10.5006/2563](https://doi.org/10.5006/2563)